Frequency Domain Model Simplification of Cumulative Mass Fraction in CMSMPR Crystallizer

Heidari, Amir; Shirvani, Mansour*+

Chemical Engineering Department, Iran University of Science and Technology (IUST)

P.O. Box16846-13114 Tehran, I.R. IRAN

ABSTRACT: *In this contribution, linearized dynamic model of Cumulative Mass Fraction (CMF) of Potassium Nitrate-Water Seeded Continues Mixed Suspension Mixed Product Removal (CMSMPR) crystallizer is approximated by a simplified model in frequency domain. Frequency domain model simplification is performed heuristically using the frequency response of the derived linearized models data. However, the CMF frequency response of the original model is obtained versus three input variables encompass seeding mass flow rate, inlet liquid volumetric flow rate and jacket temperature with emphasis on minimum model simplification assumptions. Results show that the simplified CMF frequency response predicts system dynamics and covers all system characteristics as well as the main complex model.*

KEY WORDS: *Cumulative Mass Fraction (CMF), CMSMPR crystallizer, Frequency response, Simplified model.*

INTRODUCTION

Crystallizers are one of most important equipments widely used in separation processes for production of pure materials and high-value products in process industries. In crystallization, achievement to appropriate Particle Size Distribution (PSD) is one of the important challenges for chemical engineers. Continual variations in PSD, affects physicochemical and mechanical properties of materials and complicates the design and operation of downstream process units, resulting in reduction in the efficiency of the whole plant. Complications in crystallizers mainly arise from unknown and transcendental dynamic behavior of mathematical model of system especially in population balance models.

As a process system, crystallizers can be considered as a particulate system comprised of continuous and dispersed phases [1]. Mathematically, particulate process systems are subset of hyperbolic integro-differential equations. Integral terms appear in energy, material and population balance equations. The integro-differential equations are the sources of interesting and problematic dynamic behavior in continuous processes. This behavior includes open-loop instability, long period oscillations, and slow damping of disturbances [2].

It is fully realized that the problem of synthesizing and implementing high-performance models for recognition of particulate process dynamics to achieve appropriate

PSD has significant industrial value. So, different models for controlling particulate systems to achieve desired product specifications have been developed. *Panagiotis et al.* [3] in an excellent review have provided detailed discussions of the existing results on control of particulate processes using population balance models and present an overview of future research directions in this field in the context of chemical, materials and biological process systems.

In spite of various methods available for improving control of particulate processes, there are few comprehensive studies on consideration of dynamic characteristics of these systems. Actually, the population balance or equivalently PSD is the origin of distributed parameter nature of the system which results in mathematical complications in the dynamics of the process. Nevertheless, this subject restricted high accurate dynamic analysis of particulate processes but many researchers tried to overcome this limitation in their researches.

First attempts to explain dynamic characteristics of crystallizers started in the early 1960s by *Sherwin* [4] and *Randolph* [5]. They considered cycles in fines removal and product removal crystallizer and effects of these phenomena on stability of process. *Yin et al.* [6] have investigated stability and dynamics of linearized model of a continuous crystallizer with a size-dependent crystal growth rate. They have shown that instabilities are possible over certain ranges of kinetic, physical, and operational parameters. *Motz et al.* [7] and *Vollmera & Raisch* [8] have designed stabilizing feedback controller based on stability analysis of simple model crystallizer transfer function by using H_∞ theory. Their model only describes the plant behavior but is not capable of predicting effects of changes in crystallizer design or operating conditions. *Béla et al.* [9] considered dynamic behavior of isothermal CMSMPR based on the moment equations model. They observed bifurcation behavior, quasi periodic oscillations, period doubling cascades to chaos and noise driven oscillations by applying external and internal periodic forcing to the system. *Moldoványi et al.* [10] analyzed controllability and observability of MSMPR crystallizer as well as the coupling between the inputs and the outputs by simulation using the linearized moment equation model. They showed that the crystallizer is a nonlinear MIMO system with strong coupling between the state variables.

Some of the studies on dynamics of particulate processes, especially crystallizers, are developed on the basis of frequency response evaluation. One of the excellent works regarding recognition of dynamic behavior of particulate processes and their stability is by *Ramanathan* [2], which has been done in Laplace domain. *Ramanathan* [2] analyzed stability and dynamic behavior of some particulate processes including fluidized bed calciner and isothermal CMSMPR. He discusses in detail about dynamic characteristics of these models, considering the zeroes and poles location in process transfer function and effects of them on system stability and frequency response. Because of complicate models that such processes are included, *Shirvani et al.* [11,12] in a heuristic method, developed a simplified model for statement of complex transfer function models in frequency response domain. They have shown that frequency response data of a process system provides excellent recognizable information about structure of a lumped process system as well as a distributed process system such as the crystallizer systems which can be detected clearly in a heuristic manner. The simplified structure model was validated for continues isothermal crystallizer and rotary cement kilns.

In this paper it was tried to make use of the heuristic frequency domain model simplification and parameter identification method of *Shirvani et al.* [11,12] for obtaining simplified transfer function models of CMSMPR crystallizer process for the following input variables and CMF as the output of the system.

1) Seeding mass rate ($\dot{m}_{in}$)

2) Inlet volume molar rate ($\dot{Q}_{L,in}$)

3) Jacket temperature (T_{jacket})

The paper is organized as follows. In Part A mathematical dynamic model of the process for both dispersed phase (solid phase) and continues phase (liquid phase) using population, mass and energy balances is presented. In Part B after rigorous linearization of the derived model, system frequency responses for the above mentioned input variables is obtained and then simplified transfer function models using the resulted frequency response information of the rigorous model is derived using heuristic identification method of *Shirvani et al.* [12] for determining structures as well as the parameters of the simplified models.

PART A : MODELING

Model Development

Modeling of the particulate system within a continuous crystallizer can be decomposed into two parts according to Fig. 1. The first is a binary mixture in continuous liquid phase involving dissolved crystals (solute (A)) and solvent (B). This phase determines nucleation and growth rate of crystals in crystallization process and has main effect to achieve appropriate PSD. The second is dispersed solid phase consisting individual crystals. In this phase generated crystals growth will be corresponding to degree of supersaturation that exert by liquid phase. In the following, mathematical modeling of both dispersed phase and Liquid phase for CMSMPR will be derived.

Modeling of dispersed phase

Modeling of PSD in dispersed solid phase needs to make use of population balance approach. For more information concerning this approach the reader is referred to textbook by *Ramkishna* [13]. This approach provides number density function $F(L, t)$ that can be written as follows:

$$\frac{\partial F}{\partial t} = -\frac{\partial (GF)}{\partial L} + \dot{F}_{at}^{\pm} + \dot{F}_{in} - \dot{F}_{out} - F_{dis}^{-} \qquad (1)$$

In Eq. (1) the term on the left hand side represents the accumulation of crystals with size L. The first term on the right hand side represents the convective transport in the direction of the property coordinates L due to crystal growth, where G is the crystal growth rate. The term $\dot{F}_{at}^{\pm}$ denotes source and sink terms due to particle attrition. The terms $\dot{F}_{in}$ and $\dot{F}_{out}$ denote the fluxes of inlet and the outlet particle number. Finally, it has to be taken into account that small crystals may dissolve and thus vanish from the population under certain operating conditions. This particle number flux is denoted by F_{dis}^{-}. Eq. (1) is very comprehensive and we need to take some assumptions for analytical solution of governing equations to represent the crystallizer linearized dynamics of the process. The assumptions are:

1) The term $\dot{F}_{at}^{\pm}$ can be neglected due to low agitation and low concentration of crystal particles.

2) Crystals are supposed not to dissolve in mother liquid. This means that system is always in supersaturation conditions. So, the term $\dot{F}_{dis}^{-}$ is assumed to be zero.
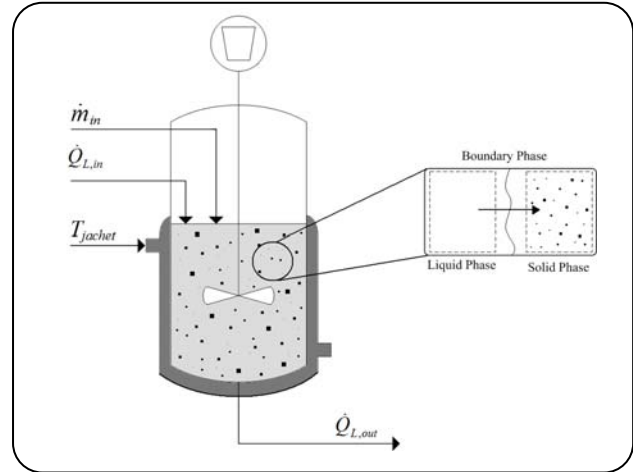

Fig. 1: Continuous crystallizer.

3) Crystal growth rate is only a function of super-saturation. Because of crystal length independency, this type of growth rate can be used in solution of governing equations by moment method.

4) Primary nucleation occurs only at L=0.

5) With the perfect agitation assumption, particle number density function in the withdrawn stream of crystallizer is assumed to be equal to the particle number density function inside the crystallizer.

The growth rate term G of the crystals is defined with different models [14]. In this study *Miller* [15] correlation for growth term in KNO_3-H_2O is used. He interpreted this term as a function of super-saturation as following:

$$G = k_g \hat{S}^q \qquad (2)$$

$$\hat{S} = \frac{\hat{C}_{L,A} - \hat{C}_{L,A,sat}}{\hat{C}_{L,A,sat}}$$

In this equation k_g and q are constants, $\hat{S}$ is the super-saturation fraction. $\hat{C}_{L,A}$ and $\hat{C}_{L,A,sat}$ are the solute concentration and the solute saturation concentration, respectively. *Ramkrishna* [13], *Rojkowski* [16] introduced initial and boundary conditions for population balance equation. *Miller* [15] developed a new model for boundary condition by using some simplifications as follows:

$$F(L = 0, t) = \frac{B_0}{G} \quad \rightarrow \quad B_0 = k_b \hat{S}^p \hat{\mu}_3 \qquad (3)$$

where B_0 is the primary nucleation rate that provides total number of nuclei generated at L=0. The symbols k_b and p are constants and $\hat{\mu}_3$ is the third moment of

Table 1: Nucleation and growth parameters [15].

Parameter	Value	Unit
k_g	5.8889×10^{-5}	m/sec
q	1.32	-
k_b	3.1859×10^8	kg solvent/(m^3sec)
p	1.78	-

PSD per kilogram of solvent. The growth and nucleation parameters for KNO_3-H_2O crystallization system are evaluated by *Miller* [15] and are listed in Table 1. In this study the boundary condition that was defined in Eq. (3) is used for modeling.

Based on the assumption 5, the following relation holds for the particle number flux due to product removal:

$$\dot{F}_{out}(L,t) = \frac{F(L,t)}{\tau} \quad \rightarrow \quad \tau = \frac{V}{\dot{Q}_{L,in}} \tag{4}$$

Where symbols τ, V and $\dot{Q}_{L,in}$ are the crystallizer residence time, the volume and the inlet liquid volumetric flow rate, respectively. The initial condition for Eq. (1) is defined as:

$$F(L, t = 0) = 0 \tag{5}$$

Eqs. (1) - (5) are mathematical description of the dispersed solid phase *S,* for continues crystallizer. The next subsection deals with the modeling of the continuous liquid phase.

Modeling of continuous phase

The fundamental balance equations for the continuous liquid phase are components mole balance for dissolved crystals (component A) and solvent (component B). During the crystallization it is assumed that the content of liquid phase is ideally mixed and formed crystals are solvent free (pure component A). Therefore, mole balances for continuous phase are:

$$\frac{dn_{L,A}}{dt} = -\dot{n}_{nu} - \dot{n}_{gr} + \dot{n}_{A,in} - \dot{n}_{A,out} \tag{6}$$

$$\frac{dn_{L,B}}{dt} = \dot{n}_{B,in} - \dot{n}_{B,out}$$

The first term in the right hand side of solute component balance $\dot{n}_{nu}$ shows the total molar exchange flux between the solid and the liquid phase due to primary nucleation rate. This term, on basis of fourth assumption does not affect on balance equation and is put equal to zero. The second term $\dot{n}_{gr}$ shows the total molar exchange flux between the solid and the liquid phase due to growth rate and can be derived as:

$$\dot{n}_{gr} = \frac{3k_v\rho_S}{M_S} \int_0^{L_\infty} L^2 GF(L,t)\, dL \tag{7}$$

The symbols, k_v, ρ_S and M_S are the volume shape factor, the solid density and the molar mass of solid phase, respectively. The terms $\dot{n}_{A,in}$ and $\dot{n}_{B,in}$ are the inlet molar flow rate of components A and B, respectively. The terms $\dot{n}_{A,out}$ and $\dot{n}_{B,out}$ denote the outlet molar flow rate of components A and B. They are defined based on the assumption (5) as a following:

$$\dot{n}_{A.out} = \frac{n_{L,A}}{\tau} \quad , \quad \dot{n}_{B.out} = \frac{n_{L,B}}{\tau} \tag{8}$$

The initial conditions for Eq. (6) are defined as follows:

$$n_{L,A}(t=0) = n_{L,A_0} \quad , \quad n_{L,B}(t=0) = n_{L,B_0} \tag{9}$$

The symbol n_{L,A_0} and n_{L,B_0} respectively are the initial number of solute and solvent moles in crystallizer. In crystallization process, because of dependence of super-saturation on temperature, furthermore exothermic nature of crystallization process and also influence of jacket temperature on crystallizer contents temperature, Eqs. (1) and (6) should be coupled with energy balance. In the next section energy balance will be derived as one of the governing equations.

Energy balance

In crystallization process, product quality has high dependency to amount of nucleation and growth rate. On the other hand these parameters are severely functions of crystallizer temperature. Thus, temperature behavior should be considered in analysis of processes dynamics. For consideration of crystallizer temperature behavior, energy balance should be coupled with component mole

balances and population balance. For CMSMPR crystallizer energy balance is as following:

$$n_{cr}c_{p,cr}\frac{dT_{cr}}{dt} = -\Delta H_{crystal} \times \dot{n}_{gr} + \quad (10)$$

$$c_{p,in}(\dot{n}_{A,in}+\dot{n}_{B,in})\times(T_{in}-T_{cr})+Q_{cool}+W_{stirrer}$$

I.C. $T_{cr}(t=0)=T_{cr_0}$

The symbols n_{cr} and $c_{p,cr}$ are total mole numbers and heat capacity of crystallizer contents and the symbols $\Delta H_{crystal}$ and $c_{p,in}$ in the right hand side are heat produced due to crystallization and heat capacity of total inlet components, respectively. In this study because of low effect of crystals on crystallizer and inlet flow heat capacity, the terms $c_{p,cr}$ and $c_{p,in}$ are considered to be only a function of solution heat capacity. The symbol Q_{cool} is the amount of heat that transfers between crystallizer and coolant and is calculated as:

$$Q_{cool} = UA \times (T_{jacket} - T_{cr}) \quad (11)$$

The terms UA and T_{jacket} are the overall heat coefficient and the jacket temperature, respectively. The energy dissipation rate of the stirrer $W_{stirrer}$ is correlated by *Gahn & Merssman* [17] and is given by:

$$W_{stirrer} = 0.3\rho_L\omega_{stirrer}^3 d_{stirrer}^5 \quad (12)$$

where ρ_L, $\omega_{stirrer}$ and $d_{stirrer}$ are liquid density, angular speed and diameter of stirrer. In this contribution we suppose that coolant temperature does not change during the operation. So, the energy balance for coolant is not needed. Eqs. (1) - (10) are dynamic model description of a CMSMPR system.

To solve and simulate the developed model, KNO_3-H_2O system is selected. In the next section physical and chemical properties of this system accomplished by operational conditions will be presented.

Physical properties and geometries

The required physical and all geometrical parameters and operational conditions for the process selected in this paper are taken from *Gerstlauer et al.* [18] and *Miller* [15]. Heat of crystallization and solubility of KNO_3 in water are respectively:

$$\Delta H_{crystal} = -20484 + 22173.1 \times \hat{C}_{L,A} + 23881 \times \hat{C}_{L,A}^2 \quad (13)$$

$$\hat{C}_{L,A,sat} = 0.1286 + 0.00588 \times T_{cr} + 0.0001721 \times T_{cr}^2$$

Table 2: Physical properties for potassium nitrate (KNO₃) and water (H₂O) [18].

Parameter	Value	Unit
k_V	$\pi/6$	-
M_A, M_S	101.103×10^{-3}	kg / mol
M_B	18.0152×10^{-3}	kg / mol
ρ_B	987	kg / m³
ρ_S	2109	kg / m³

Table 3: Operating conditions for the continuous Crystallizers [18].

Parameter	Value	Unit
V	7.5×10^{-3}	m³
$\omega_{stirrer}$	650	Cycle/min
$d_{stirrer}$	0.1	m
$c_{in,A}$	3.4×10^3	mol/m³
$x_{L,A,in}$	0.0683	-
$T_{in}, T_{jacket}, T_{cr_0}$	298.15	K
$x_{L,A,0}$	$x_{L,A}(T_{cr})$	-
$\dot{m}_{seed,in}$	0.005	kg/s

All the other physical parameters and required operating conditions are listed in Tables 2 and 3.

Simulation

Solution of governing equations is performed by the use of moment method. The moment method converts integro-differential PDE form of population balance model to a set of ODE equations. *Shervin et al.* [4] suggested this method for population balance models when growth term either is not a function of crystal length or is a first order function of the length. In this paper because of independence of growth rate to the crystal length and also dependence of nucleation term to third moment, method of moment has been selected for solution of governing equations. By applying this method to Eqs. (1), (6) and (10) the governing equations are defined as following:

$$\frac{d\mu_0}{dt} = (1 - k_V\mu_3) \times B_0 + \dot{\mu}_{0,in} - \mu_0/\tau \tag{14}$$

$$\frac{d\mu_1}{dt} = G \times \mu_0 + \dot{\mu}_{1,in} - \mu_1/\tau$$

$$\frac{d\mu_2}{dt} = G \times \mu_1 + \dot{\mu}_{2,in} - \mu_2/\tau$$

$$\frac{d\mu_3}{dt} = G \times \mu_2 + \dot{\mu}_{3,in} - \mu_3/\tau$$

$$\frac{dn_{A,L}}{dt} = -\frac{3k_V\rho_s}{M_s} \times G \times \mu_2 + \dot{n}_{A,in} - \dot{n}_{A,out}$$

$$n_{cr}c_{p,cr}\frac{dT_{cr}}{dt} = -\Delta H_{cr} \times \left(\frac{3k_V\rho_s}{M_s} \times G \times \mu_2\right) + Q_{cool} + W_{stirrer}$$

Where μ_i is the ith moment and is defined as:

$$\mu_i = \int_0^{L_\infty} L^i F \times dL \tag{15}$$

Where μ_0, μ_1, μ_2 and μ_3, are the number, the length, the surface and the volume of total crystals, respectively. Symbols $\dot{\mu}_{0,in}$, $\dot{\mu}_{1,in}$, $\dot{\mu}_{2,in}$ and $\dot{\mu}_{3,in}$ are the crystallizer inlet moments and calculated by moment definition as following:

$$\dot{\mu}_{i,feed} = \int_0^{L_\infty} L^i \dot{F}_{in} \times dL \tag{16}$$

The inlet stream PSD is assumed to be equally distributed between $L_{in,min}$ and $L_{in,max}$ and is evaluated as:

$$\dot{F}_{in} = 4 \times \frac{\dot{m}_{in}}{k_v\rho_s(L_{in,max}^4 - L_{in,min}^4)} \times \tag{17}$$

$$\left(\text{Heaviside}\,(L - L_{in,min}) - \text{Heaviside}\,(L - L_{in,max})\right)$$

Where $\dot{m}_{in}$ is the inlet mass flow rate of particles. The set of ordinary differential equations in Eq. (14) is solved by using the fourth order of Runge-Kutta numerical method in four different inlet conditions presented in Table 4. Simulation results are shown in Figs. 2 and 3. These figures respectively show first moment behavior and solute A concentration with crystallizer temperature versus time for presented systems in Table 4.

In crystallizer modeling using a simple algebraic model for description of population density function F behavior, provides reduction in computational time for the system. In this contribution Log-Normal (L-N)

Table 4: Systems conditions.

	$\dot{m}_{in}$,(kg/s)	$Q_{in}\,(m^3/s)$	$T_{cr}(K)$
System 1	0	4.17×10^{-6}	289
System 2	0.001, ($L_{in,min}$=50 μm and $L_{in,max}$=160 μm.)	4.17×10^{-6}	289
System 3	0	6.17×10^{-6}	289
System 4	0	4.17×10^{-6}	288

distribution function has been used for calculation of population density function F. This function provides a reliable model for prediction of size distribution on basis of moments values [19]. The Log-Normal distribution function is described by:

$$F_{L-N}(t,L) = \frac{1}{\sqrt{2\pi}L\ln\sigma} \times \exp\left(-\frac{(\ln L - \ln u)^2}{2(\ln\sigma)^2}\right) \tag{18}$$

Where u is the geometric mean number and σ is the geometric standard deviation. Applying the L-N distribution to the moment relation, Eq. (15), the relation between each moment is represented by expression:

$$\mu_i = u^i \exp\left(\frac{i^2}{2}(\ln\sigma)^2\right) \tag{19}$$

The characteristic parameters u and σ of L-N distribution can be derived by use of first order and second order moments as:

$$u(t) = \frac{\mu_1^2}{\sqrt{\mu_2}} \qquad , \qquad \sigma(t) = \exp\left(\sqrt{\ln\left(\frac{\mu_2}{\mu_1^2}\right)}\right) \tag{20}$$

Now by evaluation of u and σ, L-N distribution function F can be evaluated. Fig. 4 demonstrates evaluated population density by L-N distribution function in steady state condition for presented systems in Table 4. In operational conditions of systems 1,3 and 4 which there is not any particle in feed, there are wide range of PSD in the crystallizer and outlet flow. On the other hand, when specified crystal particles are inserted in the feed stream, system 2, we will have a narrow PSD during crystallizer operation. Such different behavior in PSD between systems 1, 3 and 4 with the system 2 is obviously due to presence of crystals in feed stream.
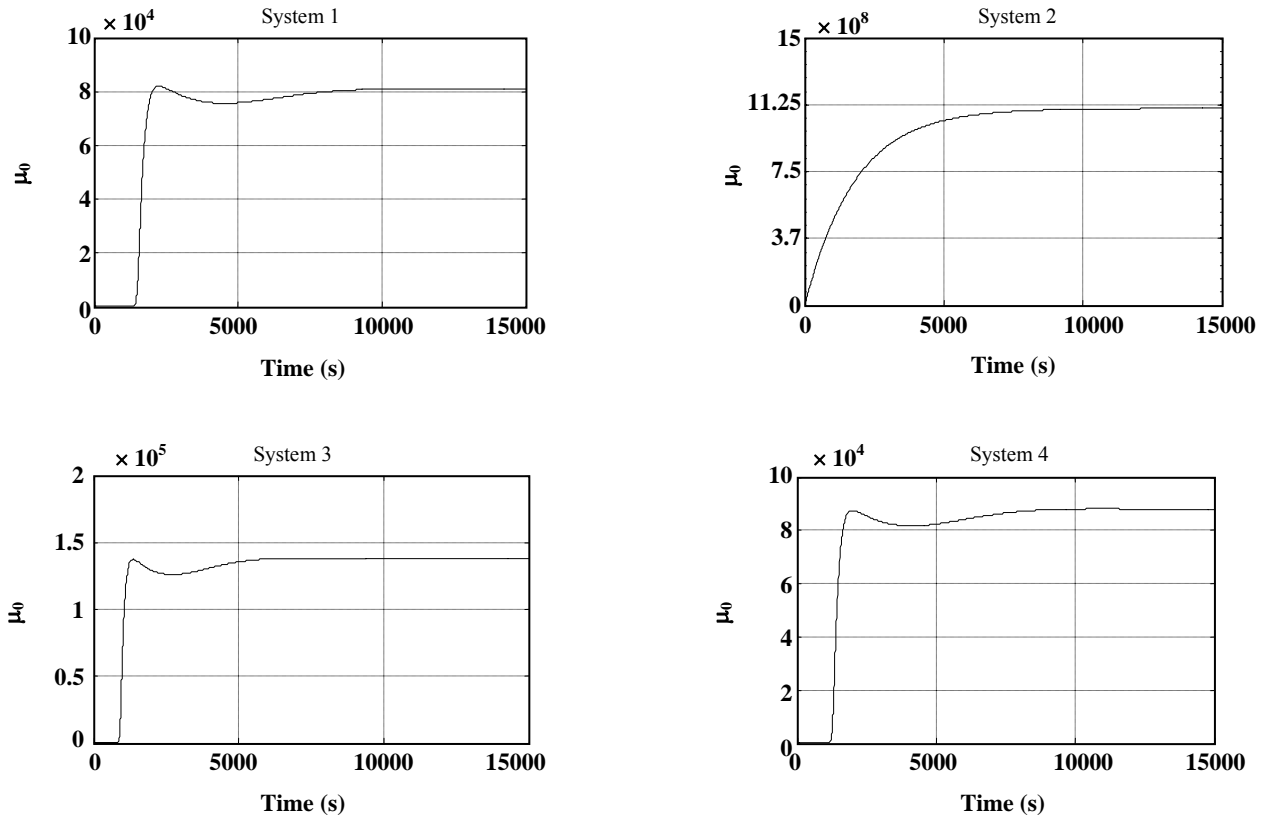
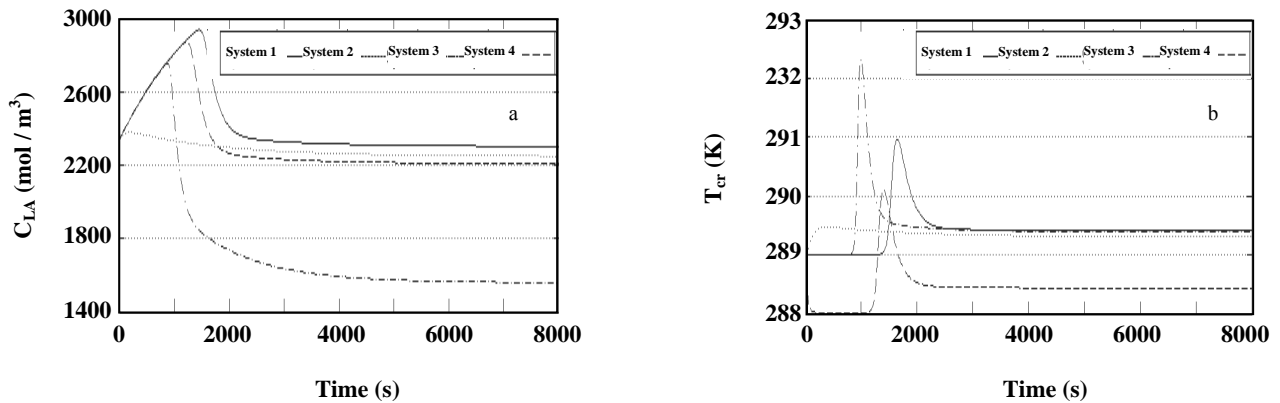*Fig. 2: Simulation results of first moment for presented systems in Table 4.*

Fig. 3 : a) KNO$_3$ concentration $C_{L,A}$ in four different operational conditions presented in Table 4,
b) crystallizer temperature T_{cr} in four different operational conditions presented in Table 4.

With a specific amount of particles in the feed stream, the driving force, i.e., supersaturation in crystallizer is significantly decreased for growth of particles and prevents from high nucleation rate during crystallizer operation. This is because of higher sensitivity of growth term on supersaturation with respect to nucleation term.

It should be mentioned that, owing to presence of noticeable number of particles in feed stream, in the system 3 (the system which includes inserted particles in the feed stream) and division of driving force between these crystal particles, we have small shift in PSD of product stream with respect to feed stream PSD.
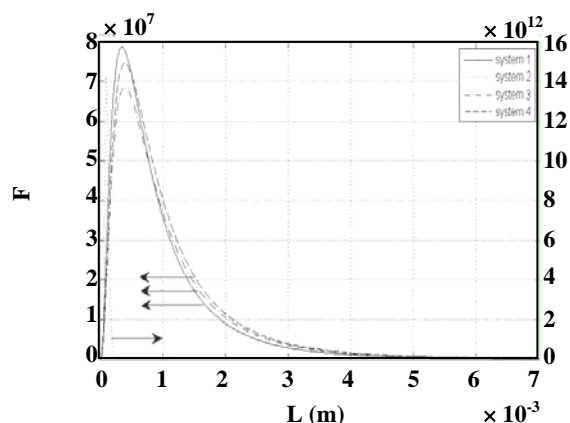
Fig. 4: PSD at steady state condition (t_s=1000 sec) for presented systems in Table 4.

In the other three systems, i.e., systems 1, 3 and 4, growth and nucleation kinetics are relatively in equal competition for consuming the crystallizer super-saturations. So there is a wide range of PSD in these systems.

According to the simulation results, Fig. 2 through Fig. 4, the selected parameters for investigating system behavior represent considerable effect on system dynamics, especially on PSD of the product. So, these parameters can be selected as manipulating variables for controlling system to achieve desirable product.

One of the most important problems in control of crystallizers is the choice of an appropriate criterion for measurement of PSD. Utilizing direct methods for PSD measurement need expensive image processing equipment that is not a reasonable way for PSD counting. The best way to solve this problem is to select an indirect criterion for evaluation of PSD such as CMF. The CMF is a suitable criterion that is widely used in industry for determining particle size distribution. Unlike the other parameters for evaluating PSD, such as nuclei density, the CMF does not require to count particles within different size fractions. Measurement of the CMF requires separating the sample into a few fractions and weighting them. This operation can be automated with existing solid handing equipments like sampling, classifying (sieve or cyclone) and automated weighting devices [2]. The dimensionless CMF above the cut point size is defined as:

$$M_c = \frac{\int_{L_c}^{\infty} L^3 F(L, t)\, dr}{\int_{L_c}^{\infty} L^3 F(L, t_s)\, dr} \tag{21}$$

Where symbol L_c and t_s are the cut-point size and system steady state time, respectively. In this study the system reached to steady condition at $t_s \approx 10000$ sec .

In part B of the paper due to importance of CMF dynamic behavior in control of crystallizer, frequency response of linearized CMF transfer function is presented. A heuristic frequency domain model simplification method developed by *Shirvani et al.* [12] is used for predicting simplified structure of CMF transfer functions of the crystallizer from the frequency response data of the original linearized model. This method, because of recognition of higher important terms in crystallizer dynamic and simplicity in its form, increases control system performance during disturbances rejection. Results show excellent ability of the simplified models in describing the dynamics of the system.

PART B

In this part after providing a brief overview about dynamic characteristics of particulate processes, linearization of governing Eq. (14) and the population balance Eq. (1) around steady state point is presented. Subsequently, regarding different input variables, CMF transfer function is derived. Finally, using frequency response data of the main derived linearized CMF transfer function, the simplified transfer functions for description of CMF variations with respect to different input variables is obtained.

Dynamic of particulate processes

The dynamics of a large class of process systems have been modeled by hyperbolic partial differential equations. Particulate processes are one subsets of this class that have complex behaviour in control problems [2].

In Laplace domain, theses processes have transfer function with infinity of zeros that may locate partially or totally in right half or left half of the complex plane. In the case of appearance of right half plane zeros larger phase lags results in difficulties in controlling the system. Particulate processes transfer function in some operational and system physical conditions do not exhibit the exact delayed response characteristic of lumped parameter systems with time delay. This is due to the

above mentioned characteristic of location of zeros. Some of these transfer functions exhibit non-minimum phase behavior and if they are included in closed-loop control system yields oscillatory responses with poor performance and poor stability with PID controllers [2].

According to *Ramanathan* [2], systems with complex transfer functions that appear in hyperbolic process systems can be approximated very well with appropriate and simple transfer functions. *Shirvani et al.* [12] developed a heuristic and appropriate method in frequency domain to determine the structure of complex model as the main characteristic of the model does not ommit. In the next subsection this method is used to identify the simplified transfer functions for CMSMPR crystallizers.

Model linearization and CMF transfer function

In this part, CMF transfer functions of crystallizer as an appropriate criterion for survey of system behavior is selected. For evaluation of CMF in Laplace domain, the sets of Eq. (1) and Eq. (14) should be linearized at the steady state point. In the linearized model of Eq. (1), population balance density function at steady state point should be approximated by a function such that analytical integration of linearized model becomes possible. In this study the first order Gaussian model is used for prediction of population balance density function in steady state condition because of its ability to show PSD as well as L-N function. The general form of Gaussian model is given by:

$$\text{Gaussian} = \sum_{i=1}^{n+1} a_i \exp\left[\left(\frac{L - b_i}{c_i}\right)^2\right] \qquad (22)$$

where a is the amplitude, b is the centroid (location), c is related to the peak width, n is the number of peaks to fit and $1 \leq n \leq 8$. In this work only at n=0 analytical solution of linearized Eq. (1) is possible. The other parameters of Gaussian equation are evaluated by fitting the model on L-N distribution function at steady sate point. Table 6 shows model parameters.

Laplace transform of linearized Eq. (1) gives:

$$G \times \frac{\partial F(L,s)}{\partial L} = -F(L,s) \times s - \qquad (23)$$

$$\left(F_s(L) \times \frac{\dot{Q}_{L,in}}{V} + F(L,s) \times \frac{\dot{Q}_{L,in,s}}{V}\right) + \dot{F}_{in}(L,s)$$

$$\text{B.C} \rightarrow \quad F(0,s) = \frac{\mu_3(s)}{G}$$

where,

$$F_s(L) = a_1 \exp\left[\left(\frac{L - b_1}{c_1}\right)^2\right] \qquad (24)$$

where F_s and $Q_{in,s}$ respectively are the PSD and the inlet volumetric flux at steady sate point. In Eq. (23), because of the boundary condition dependence to $\mu_3(s)$, linearized form of Eq. (14) should be solved analytically in Laplace domain. So, $\mu_3(s)$ is obtained as:

$$\mu_3(s) = \frac{\sum_{i=0}^{6}\left((\alpha_i s^i) \times \dot{Q}_{L,in}(s) + (\alpha_i' s^i) \times \dot{m}_{in}(s)\right)}{\sum_{i=0}^{7}(\alpha_i''' s^i)} + \qquad (25)$$

$$\frac{\left(\sum_{i=0}^{5}(\alpha_i'' s^i)\right) \times T_{jacket}(s)}{\sum_{i=0}^{7}(\alpha_i''' s^i)}$$

Where $\alpha, \alpha', \alpha''$ and α''' are constant and dependent on operating point of linearization. Due to large size and complex and form of the achieved equation it is presented as a generalized equation for further simplification.

The CMF transfer function is obtained by Laplace transform of Eq. (21) as a following:

$$M_c(s) = \frac{\int_{L_c}^{\infty} L^3 F(L,s)\, dr}{\int_{L_c}^{\infty} L^3 F(L,t_s)\, dr} \qquad (26)$$

By substitution of obtained μ_3 in Eq. (14) and analytical solution of F in Eq. (23) and substitution F in Eq. (26), CMF transfer function will be evaluated. This transfer function has long terms and is very complicate. General form of obtained CMF transfer function is as following:

$$M_c(s) = \sum_{w=1}^{u} \left[\frac{\prod_{i=1}^{k} \left[\sum_{j=1}^{n} \left(a_j s^j\right) \times \exp(\tau_i s) \right]_i}{\prod_{l=1}^{m} \left[\sum_{p=1}^{q} \left(b_p s^p\right) \right]_l} \right]_w \times \dot{Q}_{in}(s) + \quad (27)$$

$$\sum_{w'=1}^{u'} \left[\frac{\prod_{i'=1}^{k'} \left[\sum_{j'=1}^{n'} \left(a'_{j'} s^{j'}\right) \times \exp(\tau'_{i'} s) \right]_{i'}}{\prod_{l=1'}^{m'} \left[\sum_{p'=1}^{q'} \left(b'_{p'} s^{p'}\right) \right]_{l'}} \right]_{w'} \times \dot{m}_{in}(s) +$$

$$\sum_{w''=1}^{u''} \left[\frac{\prod_{i''=1}^{k''} \left[\sum_{j''=1}^{n''} \left(a''_{j''} s^{j''}\right) \times \exp(\tau''_{i''} s) \right]_{i''}}{\prod_{l=1}^{m} \left[\sum_{p''=1}^{q''} \left(b''_{p''} s^{p''}\right) \right]_{l''}} \right]_{w''} \times T_{jacket}$$

Where $a, a', a'', b, b', b'', \tau, \tau'$ and τ'' are constants. Results of accurate CMF transfer function have been shown in Fig. 6. In this figure CMF frequency responses for inlet volume fluxes, $\dot{Q}_{in}$, Fig. 5-a; inlet seeding rate $\dot{m}_{in}$, Fig. 5-b; and jacket temperature, T_{jacket}, Fig. 5-c are depicted. Regarding control problems, the complicate model in Eq. (27) reduces the ability of controller for fast reaction to disturbance input to the system. This is because of long time needed for numerical solution of Eq. (27). This problem especially is because of existence of integral terms in governing equations and when accurate models for description of physical and chemical phenomena are assumed, sorely reduces controller performance during operation. Therefore development of simple transfer function that has characteristics of complicate system but at a simple scheme can overcome such problems in control field. In the next section after linearized model validation with *Miller* [15] experimental data, complicated model Eq. (27) will be approximated by some appropriate simple structured models.

Linearized Model Validation

For validation of the linearized crystallizer model we use *Miller* [15] batch crystallizer condition to validate the model. The operational conditions of batch MSMPR crystallizer have been presented in Table 5. In Fig. 6

Table 5: Operating conditions for the batch Crystallizers [15].

Parameter	Value	Unit
V	7.5×10^{-3}	m^3
$\omega_{stirrer}$	475	Cycle/min
$d_{stirrer}$	0.1	m
T_{jacket}, T_{cr_0}	305.1, 304.85	K
$n_{L,0}, n_{L,A,0}$	67.2, 5.42	mol
m_{seed}	0.005 equally distributed for $L \in [190 \, \mu m; 210 \, \mu m]$	kg

Table 6: Gaussian model parameters.

Parameter	Value(with 95% confidence bounds)
a_1	8.085×10^{10}, $(7.943 \times 10^{10}, 8.228 \times 10^{10})$
b_1	1.434×10^{-4}, $(1.423 \times 10^{-4}, 1.444 \times 10^{-4})$
c_1	7.353×10^{-5}, $(7.203 \times 10^{-5}, 7.503 \times 10^{-5})$
R-square = 0.9691	

the second moment values for experimental data and linearized model have been presented during crystallizer operation time. It can be seen rather good agreement between linearized model and experimental data.

Model simplification

In the previous sections perfect model of CMF transfer function as a general form was presented. According to *Ramanathan* [2] complicated models of hyperbolic transfer functions can be approximated with simple transfer functions. *Shirvani et al.* [12] developed the heuristic method of identifying simplified models in frequency response domain. The rules and relationships for estimating the simplified model parameters have been presented in their paper.
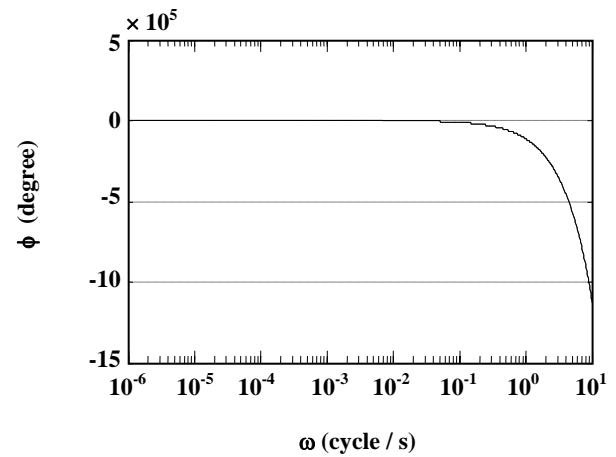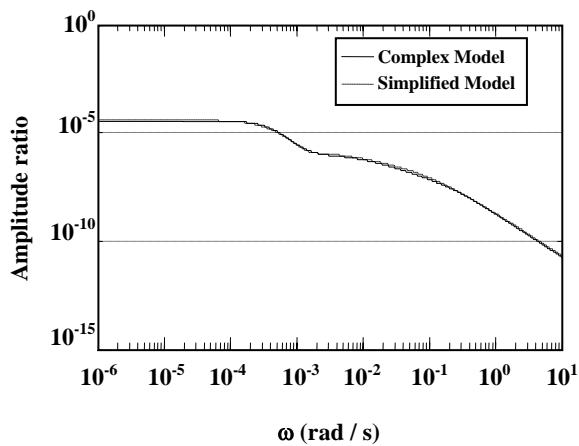
For evaluation of simplified model, CMF transfer function should be evaluated with respect to each input variables. By applying simplified model theory
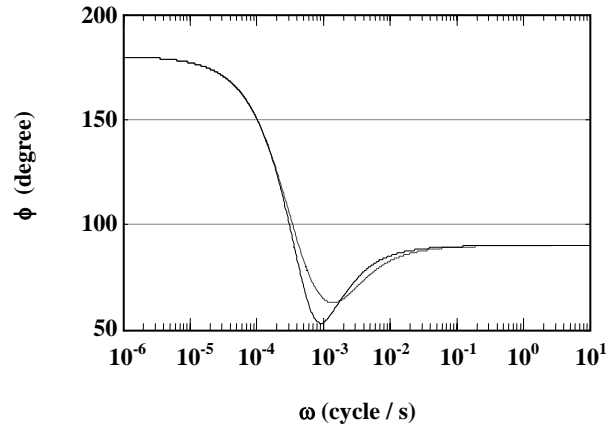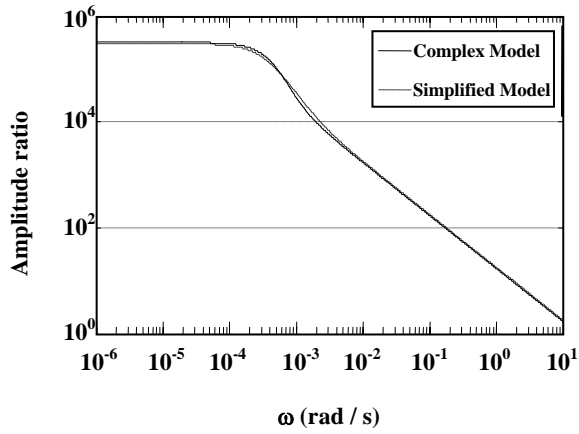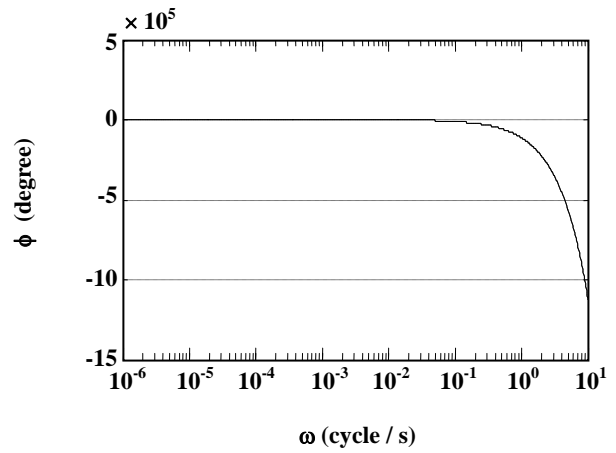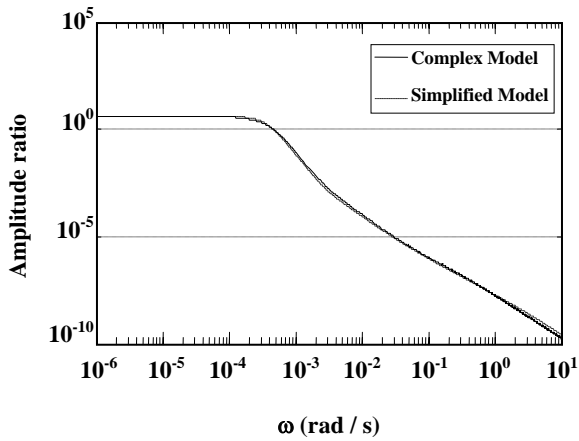
Fig. 5: CMF frequency response of simplified model and original complex model with respect to (a) $\dot{Q}_{in}$ *, (b)* $\dot{m}_{in}$ *, (c)* T_{jacket}.
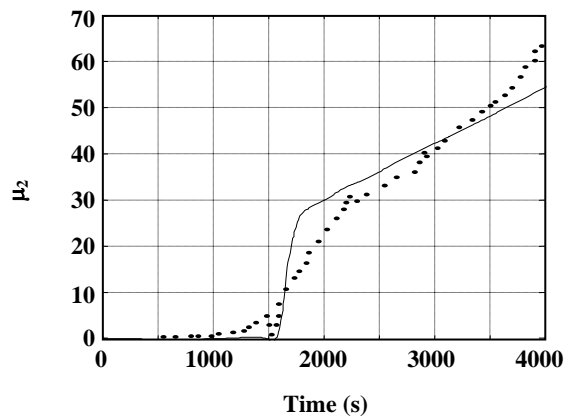
Fig. 6: Linearized model result (——) vs. experimental date (●) [15].

the simple model of CMF transfer function with respect to $\dot{Q}_{in}$ is as following:

$$M_c\big|_{\dot{m}_{in}=T_{jacket}=0} = \qquad (28)$$

$$\left(-3.9 \times \frac{(500 \times s + 1)}{(2577 \times s + 1)(3246 \times s + 1)}\right) \times \dot{Q}_{in}(s)$$

Fig. 5-a shows frequency response of simplified model Eq. (28) in comparison to the complex model, Eq. (27). The simplified model of CMF transfer function with respect to is:

$$M_c\big|_{\dot{Q}_{in}=T_{jacket}=0} = \qquad (29)$$

$$\left(\frac{-3 \times 10^{-6} \times ((370 \times s)^{1.33} + 1)}{((0.15 \times s)^{3.7} + 1)((2898 \times s)^{0.8} + 1)}\right) \times$$

$$\left(((33 \times s)^{0.8} + 1) \times \exp(-1958 \times s)\right) \times \dot{m}_{in}(s)$$

Fig. 5-b shows simplified model results of Eq. (29) with Eq. (27) and finally simplified model of CMF transfer function with respect to T_{jacket} is presented in Eq. (30) and the results is depicted in Fig. 5-c:

$$M_c\big|_{\dot{Q}_{in}=\dot{m}_{seed}=0} = \qquad (30)$$

$$\left(\frac{-3.8 \times 10^{-5} \times ((666 \times s)^{1.5} + 1)}{(3246 \times s + 1)((2570 \times s)^8 + 1)}\right) \times$$

$$\left(\frac{\exp(-1950 \times s)}{(11 \times s + 1)((10 \times s)^{0.65} + 1)}\right) \times T_{jachet}(s)$$

In Eqs. (28) through (30) simple form of CMF transfer functions have been obtained using the dominant

gain transfer function simplification of complicated transfer function models for each input variables, $\dot{Q}_{in}$, $\dot{m}_{in}$ and T_{jacket}. Afterwards, constants and powers have been modified to best fitting for each equation by least square method. Now, after evaluation of CMF transfer function with respect to individual input parameters, general form of CMF transfer function will be available by summation of right hand side of Eqs. (28) - (30). This transfer function provides an applicable and simple form of CMF dynamic behavior for analysis of system controllability during the process.

CONCLUSIONS

The method of simplification study of complex transfer function can provide a reliable technique for prediction of complex process nature. This method by recognition of the most important poles and zeroes of complex models, develop a simple model that contains dynamic characteristics of the system as well as main model.

The CMF transfer function of CMSMPR crystallizer which is one of the numerous complex transfer functions was studied in this paper. The developed simplified model for CMF provided system dynamic with respect to input parameters for recognition of influence of important parameters in dynamic behavior of CMSMPR crystallizer. Also this simplified scheme will provide high ability to take appropriate decision for choice of control method therewith decrease computation time. Results showed that the explanation of complex dynamic of CMF in CMSMPR with utilization of simplified method theory is an appropriate procedure to increase the controllability of developed complex process. The future works in concern with this study may focus on application of resultant model of CMF transfer function for controlling CMSMPR crystallizers to achieve desired particle size distribution.

REFERENCES

[1] Chiu T., Christofides P.D., Nonlinear Control of Particulate Processes, *AIChE J.*, **45,** p. 1279, (1999).

[2] Ramanathan, S., "Control of Quasi Rational Distributed Systems with Examples on Control of Cumulative Mass Fraction of a Particle Size Distribution" Ph.D. Thesis, Michigan University, (1988).

[3] Christofides P.D., Li M., Mädler L., Control of Particulate Processes: Recent Results and Future Challenges, *Powder Technol.*, **175,** p. 1 (2007).

[4] Sherwin M.B., Shinnar R., Katz S., Dynamic Behavior of the Well-Mixed lsothermal Crystallizer, *AIChE J.*, **13,** p. 1141 (1967).

[5] Randolph A.D., Beckman J.R., Krajevich Z.I., Crystal Size Distribution Dynamics in a Classified Crystallizer Part I. Experimental and Theoretical Study of Cycling in a Potassium Chloride Crystallizer, *AIChE J.*, **23**, p. 500 (1977).

[6] Yin Q., Song Y., Wang J., Analyses of Stability and Dynamic Patterns of a Continuous Crystallizer with a Size-Dependent Crystal Growth Rate, *Ind. Eng. Chem. Res*., **42**, p. 630, (2003).

[7] Motz S., Mitrović A., Gilles E.-D., Vollmer U., Raisch, J., Modeling, Simulation and Stabilizing H∞-Control of an Oscillating Continuous Crystallizer with Fines Dissolution, *Chem. Eng. Sci.,* **58**, p. 3473 (2003).

[8] Vollmer U., Raisch J., Population Balance Modelling and H∞ Controller Design for a Crystallization Process, *Chem. Eng. Sci*., **57**, p. 4401, (2002)

[9] Lakatos B.G., Blickle T., Nonlinear Dynamics of Isothermal CMSMPR Crystallizer: A Simulation Study, *Comput. Chem. Eng.*, **19,** p. 501 (1995).

[10] Moldoványi N., Lakatos B.G., Szeifert F., Model Predictive Control of MSMPR Crystallizers, *J.Cryst. Growth*, **275**, p. 1349 (2005).

[11] Shirvani M., Inagaki M., Shimizu T., Simplification Study on Dynamic Models of Distributed Parameter Systems, *AIChE J.*, **41**, p. 2658 (1995).

[12] Shirvani M., Doustary M.A., Shahbaz M., Eksiri Z., Heuristic Process Model Simplification in Frequency Response Domain, *Int. J. Eng. Transaction B*, **17**, p. 19, (2004).

[13] Ramkrishna D., "Population Balances: Theory and Application to Particulate Systems in Engineering", Academic Press, San Diego, USA, (2000).

[14] Mersmann A., "Crystallization Technology Handbook", Marcel Dekker Inc., New York, USA, (2001).

[15] Miller M.S., "Modelling and Quality Control Strategies for Batch Cooling Crystallizers" Ph.D. Thesis, Texas University at Austin, USA, (1993).

[16] Rojkowski Z., Initial Condition for Population Balance in an MSMPR Crystallizer, *AIChE J.*, **36**, p. 630 (1990).

[17] Gahn C., Mersmann A., Brittle Fracture in Crystallization Processes Part B: Growth of Fragments and Scale-up of Suspension Crystallizers, *Chem. Eng. Sci*., **54**, p.1283 (1999).

[18] Gerstlauer A., Motz S., Mitrović A., Gilles E.-D., Development, Analysis and Validation of Population Models For Continuous and Batch Crystallizers, *Chem. Eng. Sci.*, **57**, p. 4311 (2002).

[19] Sun X., Tang H., Dai J., Retrieval of Particle Size Distribution in the Dependent Model Using the Moment Method, *Opt. Express*, **15**, p. 11507 (2007).